Biomedical Microdevices (2019) 21: 38
https://doi.org/10.1007/s10544-019-0393-x

Functionalization of endovascular devices with superparamagnetic iron oxide nanoparticles for interventional cardiovascular magnetic resonance imaging

Elvin Blanco[1,2] · Victor Segura-Ibarra[1,3] · Danish Bawa[2] · Md Nafiujjaman[1] · Suhong Wu[1] · Haoran Liu[1] · Mauro Ferrari[1,4] · Alan B. Lumsden[5] · Dipan J. Shah[2] · C. Huie Lin[2]

Published online: 1 April 2019
© Springer Science+Business Media, LLC, part of Springer Nature 2019

Abstract

Presently, cardiovascular interventions such as stent deployment and balloon angioplasty are performed under x-ray guidance. However, x-ray fluoroscopy has poor soft tissue contrast and is limited by imaging in a single plane, resulting in imprecise navigation of endovascular instruments. Moreover, x-ray fluoroscopy exposes patients to ionizing radiation and iodinated contrast agents. Magnetic resonance imaging (MRI) is a safe and enabling modality for cardiovascular interventions. Interventional cardiovascular MR (iCMR) is a promising approach that is in stark contrast with x-ray fluoroscopy, offering high-resolution anatomic and physiologic information and imaging in multiple planes for enhanced navigational accuracy of catheter-based devices, all in an environment free of radiation and its deleterious effects. While iCMR has immense potential, its translation into the clinical arena is hindered by the limited availability of MRI-visible catheters, wire guides, angioplasty balloons, and stents. Herein, we aimed to create application-specific, devices suitable for iCMR, and demonstrate the potential of iCMR by performing cardiovascular catheterization procedures using these devices. Tools, including catheters, wire guides, stents, and angioplasty balloons, for endovascular interventions were functionalized with a polymer coating consisting of poly(lactide-co-glycolide) (PLGA) and superparamagnetic iron oxide (SPIO) nanoparticles, followed by endovascular deployment in the pig. Findings from this study highlight the ability to image and properly navigate SPIO-functionalized devices, enabling interventions such as successful stent deployment under MRI guidance. This study demonstrates proof-of-concept for rapid prototyping of iCMR-specific endovascular interventional devices that can take advantage of the capabilities of iCMR.

Keywords Magnetic resonance imaging (MRI) · Interventional cardiovascular magnetic resonance (iCMR) · Superparamagnetic iron oxide (SPIO) nanoparticles · Catheters · Polymer coatings

Elvin Blanco and C. Huie Lin share senior authorship.

Electronic supplementary material The online version of this article (https://doi.org/10.1007/s10544-019-0393-x) contains supplementary material, which is available to authorized users.

✉ Elvin Blanco
eblanco@HoustonMethodist.org

✉ C. Huie Lin
clin@HoustonMethodist.org

[1] Department of Nanomedicine, Houston Methodist Research Institute, 6670 Bertner Ave., Houston, TX 77030, USA

[2] Department of Cardiology, Houston Methodist DeBakey Heart and Vascular Center, Houston Methodist Hospital, 6550 Fannin St., Suite 1901, Houston, TX 77030, USA

[3] Escuela de Ingeniería y Ciencias, Tecnológico de Monterrey, 64710 Monterrey, NL, Mexico

[4] Department of Medicine, Weill Cornell Medical College, New York, NY 10065, USA

[5] Department of Cardiovascular Surgery, Houston Methodist DeBakey Heart and Vascular Center, Houston Methodist Hospital, Houston, TX 77030, USA

1 Introduction

Cardiovascular disease remains the leading cause of hospitalization and death in the US (Benjamin et al. 2018). With over one million procedures performed annually in the US (Slicker et al. 2016), cardiac catheterization remains a vital treatment modality. X-ray fluoroscopy-based cardiovascular catheterization procedures have enabled interventions that reduce the need for open surgery, including coronary angioplasty with stenting, aortic valve replacement, and atherectomy, the latter involving removal of atherosclerotic tissue from vessels (Bhat et al. 2017). However, x-ray fluoroscopy is unable to properly delineate soft tissue, relying on pre-procedural x-ray angiography, computed tomography (CT), or magnetic resonance imaging (MRI) for anatomical information (Ma et al. 2013). Poor soft tissue contrast and imaging in a single plane limits accurate navigation and positioning of endovascular tools such as catheters. Indeed, 2D fluoroscopy integrates 3D structures into a single plane, creating challenges when there are three degrees of freedom of motion in aligning an endovascular device (depicted as a screwdriver in Fig. 1) with a cardiovascular structure (depicted as a screw in Fig. 1). This loss of 3D information causes continuous misregistration errors that either prolong the procedure time or result in complications. Importantly, x-ray fluoroscopy exposes patients to ionizing radiation (Berrington de Gonzalez and Darby 2004) and iodinated contrast agents (Pucelikova et al. 2008), which can prove particularly detrimental to children born with congenital heart disease and pregnant women (Chambers et al. 2011), as well as patients with renal insufficiency. Taken together, novel approaches for imaging of cardiovascular procedures are needed to improve catheter steering and intervention, as well as patient and operator safety.

MRI-guided catheterization has tremendous transformative potential in the realm of cardiac interventional procedures by bringing together both form and function through a combination of high-resolution anatomical imaging and physiologic flow data. Cardiac MR (CMR) has superb soft tissue contrast and has the ability to obtain three-dimensional structural information and continuous imaging across multiple planes (Mazal et al. 2016). Simultaneous CMR allows the empiric measurement of blood flow through cardiovascular structures without the need for mathematical assumptions required in standard cardiac catheterization, providing superior physiological information. Consequently, interventional CMR (iCMR) enables more accurate navigation and positioning of devices, due largely to the advantage of imaging in up to three planes simultaneously. Importantly, MR imaging can highlight cardiovascular structures without the use of ionizing radiation (Bock et al. 2005), potentially reducing the risk for malignancies in patients, particularly children. Lastly, iCMR can promote the development of novel, minimally-invasive procedures that extend beyond vascular lumens, including extra-anatomic bypass, structural heart interventions, and local delivery of drugs, genes, or cells (Saikus and Lederman 2009).

While iCMR stands to bring about a true paradigmatic shift in cardiac catheterization, the modality has yet to gain widespread clinical use. A challenge exists in the form of integrating an iCMR environment in the clinical setting, including the adjacent proximity of an MRI laboratory and a fluoroscopy suite (Mazal et al. 2016). However, a significant hurdle that limits the commonplace clinical applicability of iCMR is the lack of endovascular devices suitable for CMR (Lotz 2013). Catheters currently used clinically have ferrous materials that impart the mechanical properties necessary for proper navigation and steering of the device (Ratnayaka et al. 2008). Unfortunately, these create large magnetic susceptibility artifacts due to distortion of the main static magnetic field (B_0 field) and linear nature of the frequency encoding gradient proximal to ferromagnetic objects (Stadler et al. 2007), which in turn impede proper imaging of cardiovascular structures. Of note, catheters containing materials such as nylon and polyester have been shown to possess similar mechanical properties to conventional devices containing ferrous materials (Clogenson and Dobbelsteen 2016). Research efforts have been devoted to the development of both passive and active catheters for use in iCMR. Passive catheters relying on incorporation of MRI-visible coatings or rings in the device for visualization have been explored over the last few decades (Rubin et al. 1990; Bakker et al. 1996; Omary et al. 2000; Zhang et al. 2010). Other notable examples consist of balloon-tipped devices that employ CO_2 (Miquel et al. 2004) or a T2-shortening agent (Krueger et al. 2006) to fill the balloon. Active catheters have micro-coils and circuitry that generate an MRI-visible echo upon excitation (Saeed et al. 2012), including devices containing inductively coupled radiofrequency (RF) coils (Bock et al. 2004). Balloon-tipped catheters, however, can only be used for flow-directed movement, with minimal specificity, and cannot be used for interventions. Similarly, active devices require continuous connection to an RF source, precluding this strategy for visualization of implantable devices.

Herein, our objective was to functionalize clinically-used interventional tools, including catheters, wire guides, stents, and angioplasty balloons, with a polymer coating consisting of poly(lactide-co-glycolide) (PLGA) and superparamagnetic iron oxide (SPIO) nanoparticles (NPs), in an attempt to make these devices suitable for iCMR. Following examination of commercially-available catheter-based instruments in the iCMR setting in pigs, SPIO-functionalized devices were examined and used to perform cardiovascular interventions.

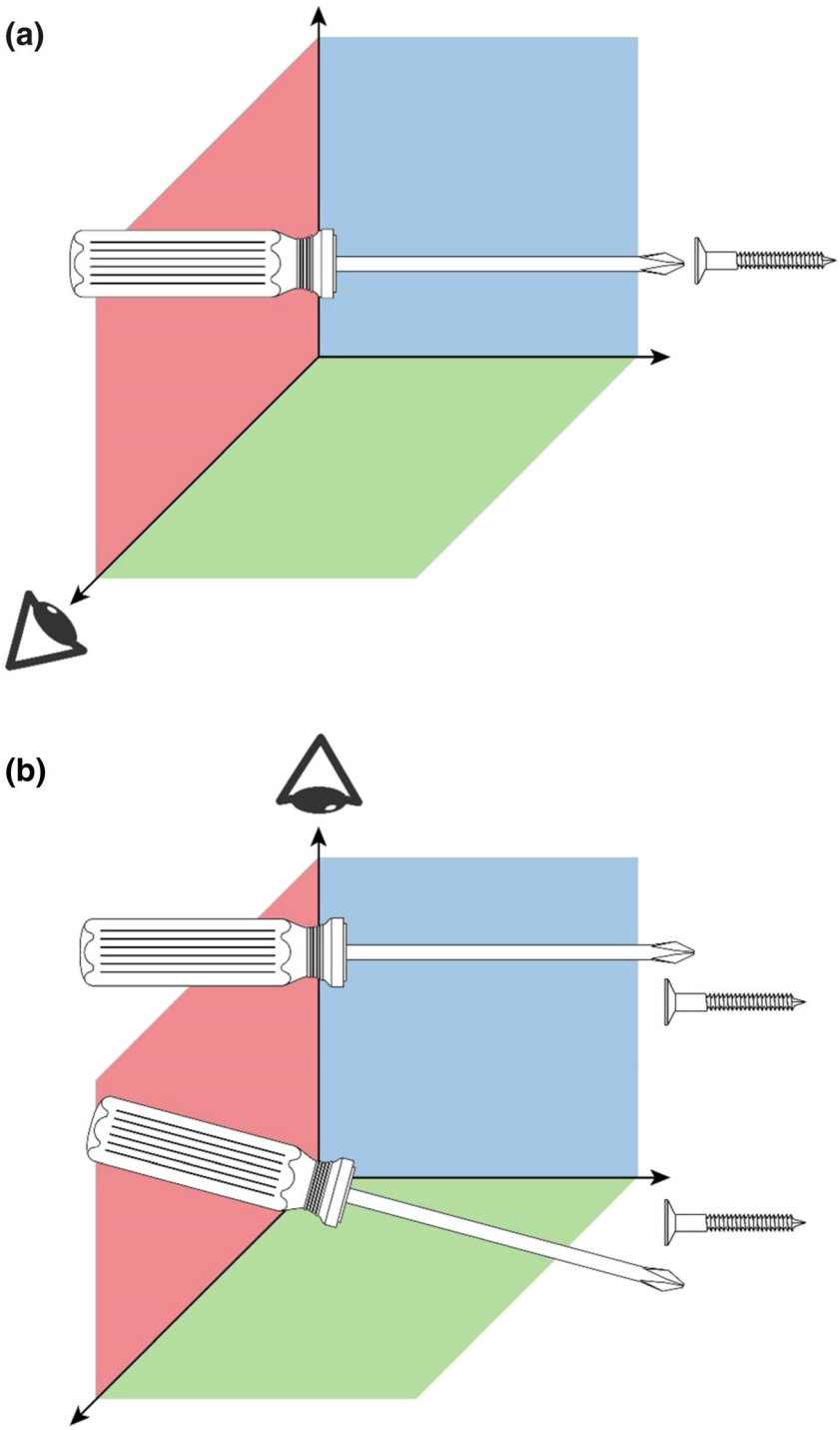

Fig. 1 Limitations of 2-D fluoroscopy for cardiovascular catheterization procedures. Due to the flattening effect of x-ray fluoroscopy, a screwdriver (endovascular device) appears aligned with a screw (cardiovascular structure) from one angle (**a**). However, an orthogonal view reveals that the screwdriver may be out of plane with the screw, or rotated off-axis from the screw (**b**). These imaging errors drive increased x-ray dose, contrast use, intervention times, and/or may require additional imaging modalities such as ultrasound or the use of preoperative computed tomography (CT) or MRI

Findings highlight the ability to properly visualize and navigate a series of SPIO functionalized endovascular instruments in cardiovascular structures, as well as successful placement and imaging of stents, with the capability to image at all stages of deployment. This study demonstrates the advantages of iCMR for endovascular procedures and the need for catheter-based tools with MRI-visible design considerations.

2 Materials and methods

2.1 Materials

Superparamagnetic iron oxide (SPIO) nanoparticles (5 nm, Lot No. 051012) were purchased from Ocean Nanotech (San Diego, CA). Ester-terminated poly(lactide-co-glycolide)

(PLGA, 50:50, 0.55–0.75 inherent viscosity) was obtained from Durect Corporation (Cupertino, CA). Clinically-used catheterization devices included the following: 1) 0.014" Hi-Torque Balance Middleweight (BMW) Universal (Abbott Vascular, Green Oaks, IL); 2) 0.014" Prowater Hydrophilic Asahi PTCA guidewire (Abbott Vascular, Green Oaks, IL); 3) 0.014" Runthrough® NS extra floppy coronary guidewire (Terumo Runthrough, Tokyo, JP); 4) 0.018" HiWire® hydrophilic wire guide (Cook Medical, Bloomington, IN); 5) 0.035" HiWire® hydrophilic wire guide (Cook Medical); 6) 7-French Arrow® balloon wedge-pressure catheter (Teleflex, Wayne, PA); 7) 14 mm × 4 cm Atlas® Gold PTA dilatation catheter (Becton Dickinson, Franklin Lakes, NJ); 8) 2.0 mm × 12 mm NC Quantum Apex™ PTCA dilatation catheter (Boston Scientific, Marlborough, MA); 9) 7 mm × 4 cm Conquest® PTA dilatation catheter (Becton Dickinson); and 10) Assurant Cobalt® balloon expandable stent system (Medtronic, Minneapolis, MN). GORE® PRECLUDE® Pericardial Membrane was obtained from Gore Medical (Flagstaff, AZ).

2.2 Polymer coating for MRI visualization

Clinically-used catheterization devices were coated with an SPIO-containing polymer solution. These included the following: 1) 0.018" HiWire® hydrophilic wire guide (Supplementary Fig. S1A); 2) 0.035" HiWire® hydrophilic wire guide; 3) Atlas® Gold PTA dilatation catheter (Supplementary Fig. S1B); 4) Apex™ PTCA dilatation catheter; 5) Conquest® PTA dilatation catheter; and 6) Assurant Cobalt® balloon expandable stent system (Supplementary Fig. S1C). SPIO NPs and PLGA, both in dichloromethane, were mixed to arrive at concentrations of 2.5, 5, and 10 mg/mL of SPIO NPs in 100 mg/mL of polymer solution. The solution was applied to the devices by brush and allowed to dry overnight. The coating on wire guides was applied specifically to the tip to allow safe visualization and navigation, whereas on balloon catheters, the coating was applied to the areas of radiopaque markers to allow for visualization of the length of the balloon. The stent delivery system was coated at the tip to optimize visualization during movement and positioning, as the stent itself could be visualized under iCMR when not in motion.

There are currently no endovascular stent grafts suitable for iCMR due to the presence of ferromagnetic metals in the delivery systems. Thus, we fabricated an endovascular stent graft system suitable for MRI use (Supplementary Fig. S2). An SPIO polymer coating was applied to a GORE® PRECLUDE® Pericardial Membrane consisting of expanded polytetrafluoroethylene (ePTFE). The Assurant Cobalt® stent was deployed and the SPIO-coated ePTFE membrane was then sutured to the exterior of the stent with 4–0 Prolene (Ethicon Inc., Somerville, NJ). Additional reinforcement was achieved using cyanoacrylate. The covered stent was then crimped on an SPIO-functionalized 14 mm × 4 cm Atlas® Gold PTA dilatation catheter.

2.3 Animal model

All animal studies were approved by the Institutional Animal Care and Use Committee of the Houston Methodist Research Institute. Male and female Domestic Yorkshire pigs (3–7 months, 35–50 kg) were used for all in vivo studies. All coated and non-coated wire guides, catheters, and balloons were each examined in two pigs ($N = 2$), with the exception of the 0.014" Hi-Torque BMW Universal, 0.014" Prowater Hydrophilic Asahi PTCA guidewire, 0.014" Runthrough® NS extra floppy coronary guidewire, 7-French Arrow® balloon wedge-pressure catheter, Assurant Cobalt® balloon expandable stent system, and the aforementioned custom endovascular stent graft system, which were each examined in one pig ($N = 1$). In each experiment, the animal was sedated with intramuscular injections of ketamine, acepromazine, and atropine. An endotracheal tube was inserted into the trachea and anesthesia maintained by administration of 1–5% isoflurane. An intravenous catheter was inserted into a marginal ear vein for fluid maintenance, and an intravenous (IV) saline solution started and continued throughout the procedure. The animal was transported to a hybrid OR/CMR suite, consisting of an adjoining catheterization lab and MRI suite present in the Houston Methodist Institute for Technology, Innovation, & Education (MITIE^{SM}, Supplementary Fig. S3), and placed in a supine position. Surgical areas were sterilized with alcohol and chlorhexidine. Vital signs were continuously monitored by the Houston Methodist Research Institute Comparative Medicine Program (CMP) vet staff throughout the procedure and documented every 15 min. Pigs were humanely euthanized upon completion of the experiment with an IV injection of phenytoin/pentobarbital combination in conjunction with an isoflorane overdose, in accordance with acceptable practices as outlined by American Veterinary Medical Association (AVMA) guidelines for euthanasia of animals.

2.4 Catheterization and MR image acquisition

Percutaneous access was performed under fluoroscopy using the Seldinger technique (Higgs et al. 2005), with introducer sheaths placed in the left and right femoral arteries and veins. Heparin (150 units/kg) was administered IV as an anticoagulant, with subsequent hourly bolus IV injections (2000–3000 units) to maintain the anticoagulation status of the animal. Animals were then transferred to the MRI suite.

Image acquisition and interventions were performed using a 1.5 T Siemens Magnetom Aera MRI Scanner (Siemens Healthineers, Erlangen, DE). Images were obtained in a series

of ECG gated 2D images in the axial, coronal, and saggital planes using a balanced steady state free precession sequence (SSFP) with typical parameters of: 1) spatial resolution 1.5–2.0 cm in plane; 2) slice thickness of 4–5 mm; and 3) flip angle of 80°, gated to mid-diastole. This was followed by an ECG gated 2D gradient echo cine with typical parameters: 1) spatial resolution 1.0–1.5 cm in plane; 2) slice thickness of 4.5 mm; 3) flip angle of 15°, 4) bandwidth of 250 Hz/pixel; and 5) temporal resolution of 30 msec per frame. Approximately 10 min following administration of the gadolinium-based contrast agent Gadobutrol (Gadavist®, Bayer Corporation, Whippany, NJ), an equilibrium phase 3-D T1 weighted gradient echo volume was acquired with typical parameters: 1) spatial resolution 1.0 mm isotropic: 2) flip angle of 10°; and 3) bandwidth of 300 Hz/pixel. Catheter manipulations were done using a real-time SSFP cine sequence with typical parameters: 1) spatial resolution of 2.0 × 2.0 mm in plane; 2) slice thickness of 8 mm; and 3) temporal resolution of 50 msec.

3 Results

Standard fluoroscopically-active catheter-based instruments are simply not suitable for use under MRI, preventing a facile translation of present-day devices into the realm of iCMR. In an attempt to highlight this limitation and demonstrate the need for MRI-visible catheters, commercially-available "off-the-shelf" catheterization devices were examined in the iCMR setting. A 0.014″ coronary wire guide with a ferromagnetic core (RUNTHROUGH® NS extra floppy coronary guidewire) produced a large artifact that obscured cardiovascular and non-cardiovascular structures in the MR image when placed in the ascending thoracic aorta (Fig. 2a), brought about by ferromagnetic metals in the wire construction. Similar massive MRI artifacts were obtained with Hi-Torque BMW and Prowater Asahi PTCA guidewires (Supplementary Fig. S4). A 0.018″ peripheral wire guide (HiWire® hydrophilic wire guide) composed of Nitinol with a tungsten-impregnated polyurethane jacket without a ferromagnetic core produced only a limited artifact in the shaft in the form of a bright signal (Fig. 2b). However, the tip of the wire guide could not be visualized in standard MRI sequences. Lastly, the Apex™ PTCA dilatation catheter, a coronary angioplasty balloon, generated a very limited signal from the radiopaque non-ferromagnetic metal ring markers (Fig. 2c).

CMR-safe balloon-tipped catheters are currently used clinically for purposes of right heart hemodynamic catheterization (Rogers et al. 2017). We examined an Arrow® balloon wedge-pressure catheter positioned at the level of the pulmonary valve, and upon inflation with a gadolinium-based contrast agent, the balloon tip was visualized in standard real-time CMR (Fig. 3a). However, the catheter shaft, and thus, the position, torque, or potential entanglement of the catheter, could not be evaluated. An adjusted saturation CMR sequence provided for enhanced visualization of the gadolinium-filled balloon, but at the expense of loss of anatomical data (Fig. 3b).

In iCMR, visualization of catheter-based devices is of paramount importance, with either limited signal or substantial artifacts proving detrimental to proper steering and positioning of catheters. We hypothesized that successful, real-time navigation of endovascular instruments is possible by applying an SPIO polymer coating to these devices. Having identified a basic toolbox of existing cardiovascular instruments that generated minimal to no MRI artifacts, these were functionalized with the SPIO polymer coating and evaluated in an iCMR setting. The dose of SPIO coating was varied in range from low concentration to a high concentration on wire guides and catheters to identify an iCMR signal that optimized both

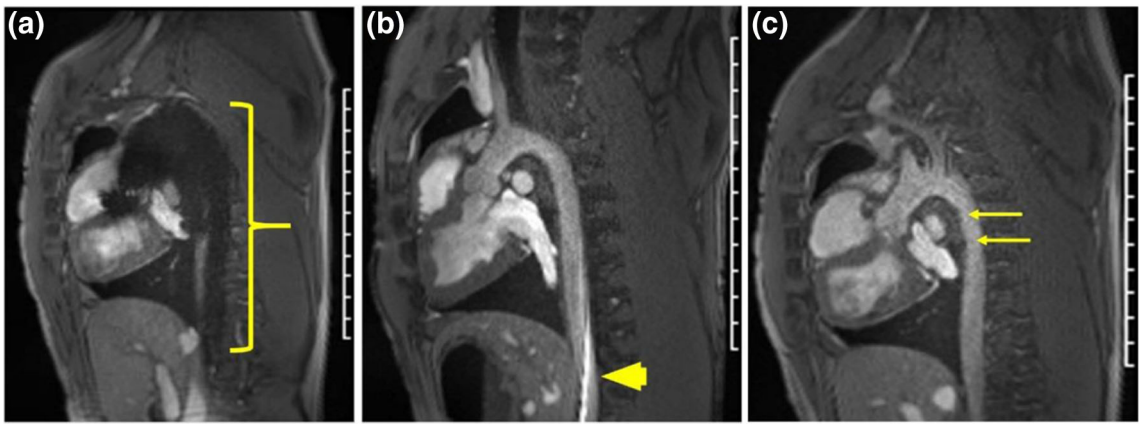

Fig. 2 CMR of "off-the-shelf" cardiovascular catheterization devices. **a** A 0.014" Runthrough® NS extra floppy coronary guidewire with a ferromagnetic core was advanced into the ascending aorta. The bracket highlights the artifact generated by the ferromagnetic core. **b** 0.018" HiWire® hydrophilic wire guide without ferromagnetic metallic components was positioned in the descending thoracic aorta. The arrowhead points to bright signal emanating from the shaft of the wire guide in the abdominal aorta. **c** An Apex™ PTCA dilatation catheter with metallic marker rings located in the descending thoracic aorta. The arrows signal the position of the marker rings. Images were obtained in gradient echo sequence

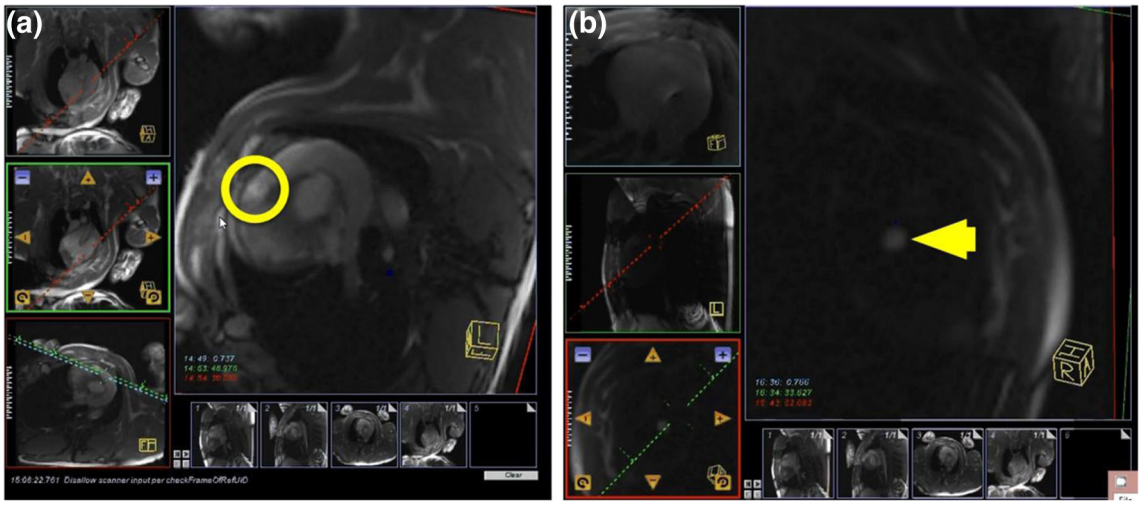

Fig. 3 iCMR of 7-French Arrow® balloon wedge-pressure catheter. **a** Balloon tipped catheter positioned at the level of the pulmonary valve and filled with diluted gadolinium-based contrast agent visualized in standard, real-time CMR. The circle indicates the tip of the catheter. Figure insets indicate multiplanar images representing 3D images acquired in real-time sequence via Interactive Front End software (Siemens Healthineers, Erlangen, DE). **b** Adjusted saturation CMR sequence highlighting enhanced visualization of gadolinium-filled balloon (arrowhead)

visibility and spatial resolution (Supplementary Fig. S5). As can be seen in Fig. 4a, the uncoated 0.018" HiWire® wire guide (the same as Fig. 2b, shown here for purposes of comparison) generated no signal at the tip of the wire guide under iCMR when positioned in the descending thoracic aorta. Upon functionalization of the wire guide, signal can be seen emanating from the SPIO-coated tip (Fig. 4b). Similarly, an ATLAS® balloon was functionalized with an SPIO polymer coating and positioned in the abdominal aorta. While the tip of uncoated controls produced a subtle signal due to the presence of metallic marker rings (Fig. 4c), the coated Atlas balloon with SPIO coating produced a very strong signal under MRI that made the balloon easily discernible without obscuring anatomy (Fig. 4d). Similar findings, wherein the catheter was easily discernible under MRI compared to uncoated catheters, were observed following SPIO functionalization of Apex™ PTCA and Conquest® PTA dilatation catheters (Supplementary Fig. S6).

Unlike steel and ferromagnetic metal containing stent platforms which create large artifact obscuring the anatomy, cobalt-based stent platforms could be visualized under iCMR when not in motion and did not obscure the anatomy (data not shown). However, visualization of the stent delivery system while in motion proved more challenging. To optimize visibility of stent delivery and deployment under iCMR, a cobalt-based device (Assurant Cobalt® balloon expandable stent system) was functionalized with an SPIO coating at the leading edge of the stent delivery system, and stent delivery was examined under MRI. This allowed visualization of the stent delivery system through the abdominal aorta (Fig. 5a), thoracic aorta, and selective positioning in the subclavian artery. The stent was then deployed in real-time via inflation of the balloon with diluted gadolinium-based contrast agent. As can be seen in Fig. 5b, the cobalt stent was successfully deployed in the subclavian artery, while the shaft of the 0.035" HiWire® wire guide was also visible in the descending thoracic aorta.

As endovascular aortic repair is an ideal target for iCMR application, our goal was then to attempt to translate endovascular stent graft technology to the iCMR setting. However, we were unable to identify any endovascular stent graft systems suitable for MRI use. To overcome this challenge, the cobalt-based balloon-expandable stent platform was modified with an SPIO-coated ePTFE membrane, giving rise to a customized iCMR-functionalized stent graft. In an attempt to highlight the ability to apply iCMR-enabled devices to cardiac interventions, the customized iCMR stent system was deployed in the pig abdominal aorta. As can be seen in the simultaneous real time MR images obtained before (Fig. 5c) and after (Fig. 5d) deployment of the stent under iCMR-guidance, the stent graft was successfully deployed in vivo in the pig abdominal aorta, best demonstrated by significant foreshortening of the device upon expansion to its final diameter.

4 Discussion

Cardiovascular catheter-based interventional procedures are currently performed under x-ray fluoroscopy, a modality associated with poor soft tissue contrast and visualization in two dimensions, limiting accurate navigation of endovascular tools (Fig. 1a). Importantly, present-day standard fluoroscopy typically requires repeated injection of iodinated contrast in order to visualize cardiovascular structures. The risk of acute renal injury related to iodinated contrast exposure frequently

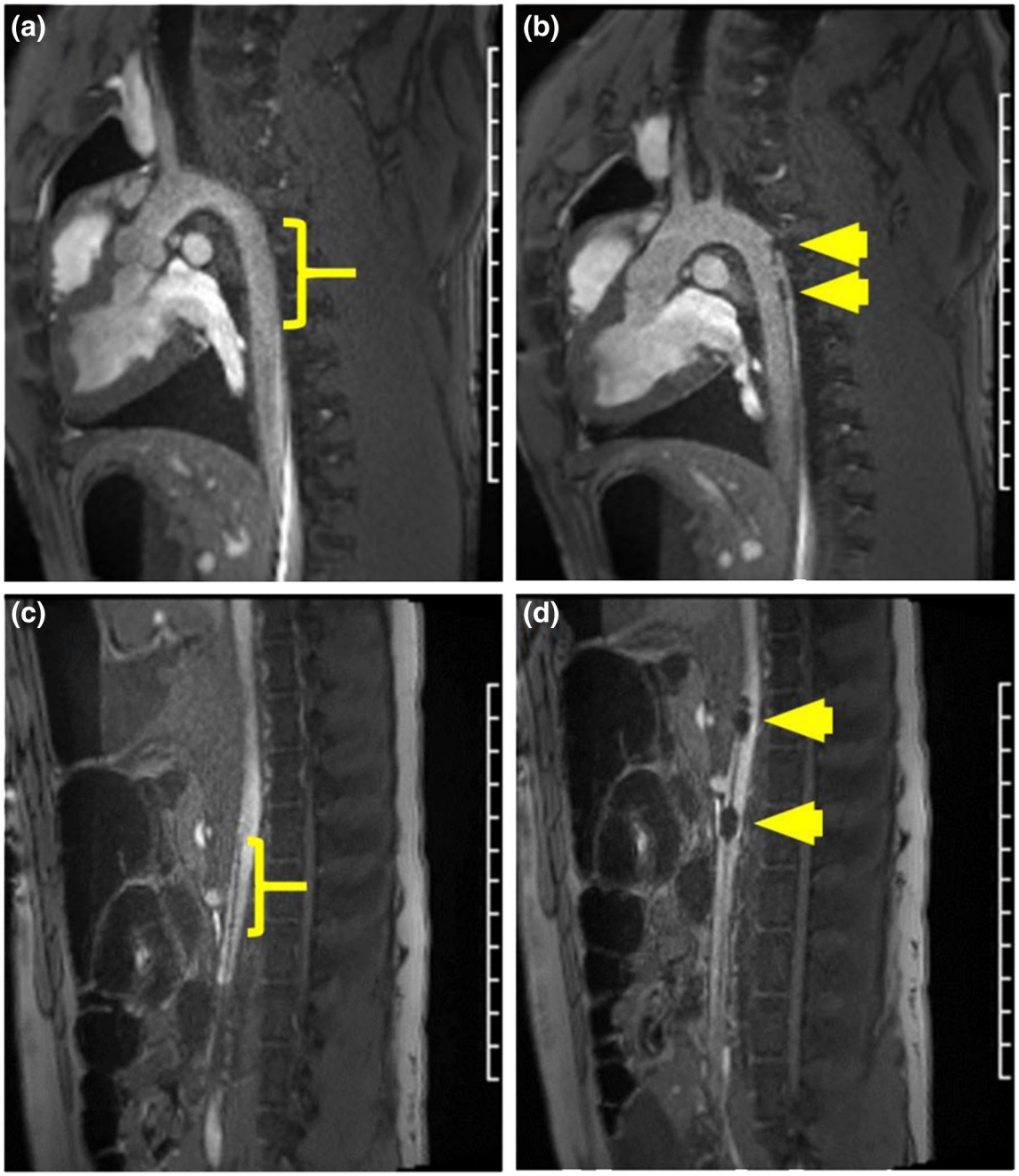

Fig. 4 SPIO functionalization of wire guide and angioplasty balloon for iCMR. **a** Control (uncoated) 0.018" HiWire® hydrophilic wire guide positioned in the descending thoracic aorta. The bracket highlights the position of the tip of the wire guide. **b** SPIO functionalized 0.018" HiWire® hydrophilic wire guide positioned in the descending thoracic aorta. Arrowheads denote the location of SPIO markers. **c** Control (uncoated) Atlas® Gold PTA dilatation catheter in the abdominal aorta. The bracket highlights signal generated by the metallic marker rings as seen on gradient echo imaging. **d** SPIO functionalized Atlas® Gold PTA dilatation catheter in the abdominal aorta. Arrowheads indicate positioning of SPIO markers

limits the use of catheterization and transcatheter intervention in patients with renal insufficiency (Andreucci et al. 2017). The inability to visualize cardiovascular structures or devices with depth lengthens the duration of complex catheterization cases, further increases x-ray and contrast exposure, reduces the likelihood of success, and may even augment the risk of complications.

MRI-guided catheterization combines high-resolution anatomical imaging with superior soft tissue contrast and physiologic flow data. Three-dimensional structural information and imaging across multiple planes enables more accurate positioning of endovascular devices in iCMR (Fig. 1b), in a setting free of radiation and harmful side effects to patients. Thus, there exists a monumental potential for iCMR to shift

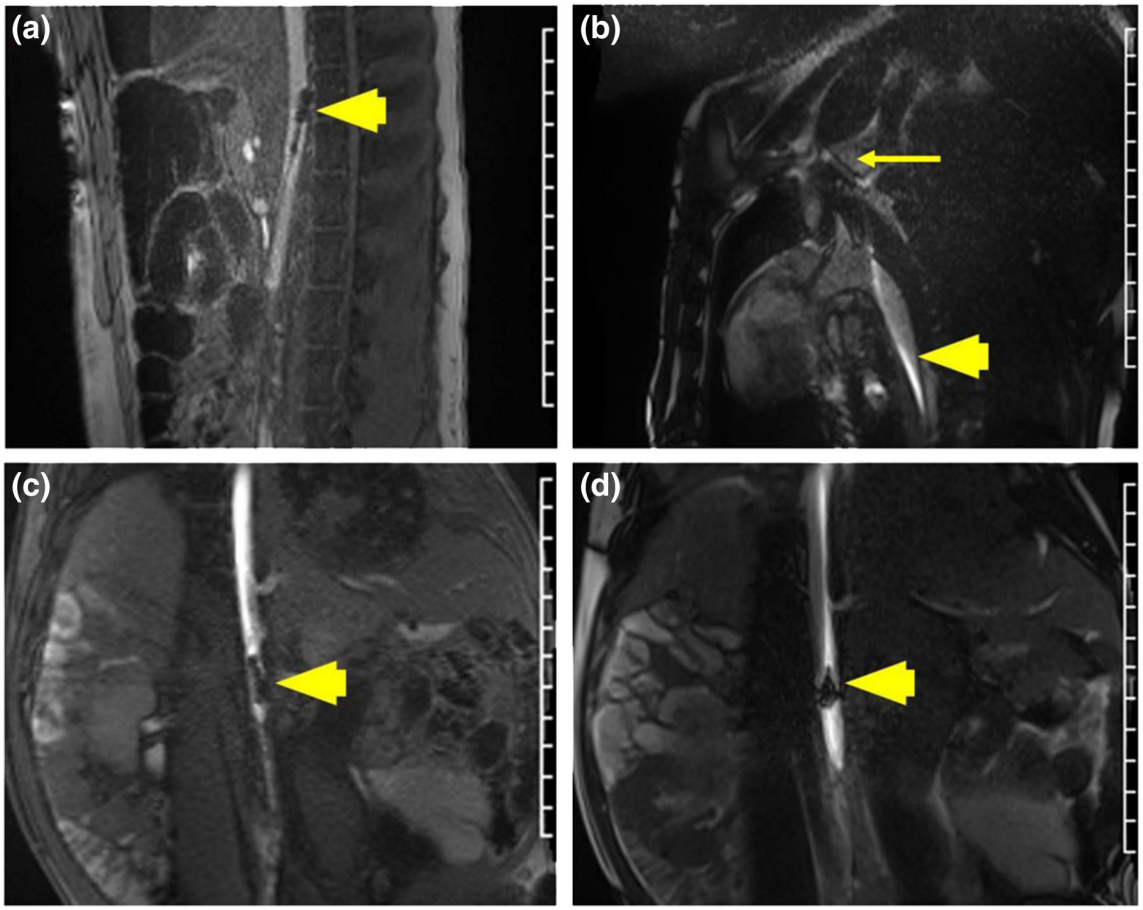

Fig. 5 Stent deployment in iCMR. **a** Assurant Cobalt® balloon expandable stent system advanced to the abdominal aorta. The tip of the catheter, which has been coated with SPIO, is denoted by the arrowhead. **b** Cobalt-based stent (arrow) deployed in the subclavian artery. The shaft of the wire guide can be seen in the descending thoracic aorta (arrowhead). Pre- (**c**) and post-deployment (**d**) of a custom endovascular stent graft system suitable for MRI use in the abdominal aorta under iCMR. The system was composed of a SPIO-coated ePTFE membrane sutured onto a cobalt balloon-expandable stent, which in turn was crimped on an Atlas® Gold PTA dilatation catheter. After deployment of the stent in the abdominal aorta, a significant foreshortening of the stent material (arrowhead) was observed

the paradigm of transcatheter interventions. It is important to note that while currently, diagnostic right heart catheterization in CMR could potentially be performed in any MRI environment that can be rendered a sterile procedure room with an invasive hemodynamic monitoring system, at present, the ability to begin to explore interventional applications clinically is extremely limited due to the non-existence of a basic toolkit suitable for iCMR. As such, the objective of this study was to determine the limitations of existing cardiac catheterization devices in the iCMR environment, and then functionalize a basic set of existing endovascular instruments using an SPIO coating, so as to realize the potential of iCMR. Specifically, we aimed to functionalize wire guides, angioplasty balloon catheters, a guiding catheter, and a stent delivery system for use in iCMR.

Herein, we demonstrated that standard wire guides used for percutaneous coronary intervention, as well as coronary diagnostic and guiding catheters, were not suitable for iCMR due to the profound artifact created by the ferromagnetic metallic braiding in these devices that obstruct visualization of anatomical structures (Fig. 2a, Supplementary Fig. S4). Moreover, ferrous material in catheters may even generate heat in the MRI environment (Klemm et al. 2000). These metallic braidings are crucial design considerations for properties (e.g. torqueability) necessary for proper device steering, and exclusion of these comes at the cost of mechanical performance (Saikus and Lederman 2009). Thus, design of catheters suitable for MRI use not only have to account for the incorporation of MRI-visible components, but also overcome the challenge of ensuring that novel catheter designs maintain specific mechanical properties essential to proper device navigation and positioning. Krueger et al. developed a non-metallic, fiber-reinforced material for use in guidewires, with mechanical properties that were similar to a Nitinol-based guidewire (Krueger et al. 2008). Of note, incorporation of iron powder particles, ranging in diameter from 6 to 8 μm, allowed for visualization under MRI.

In this study, we also examined the iCMR performance of a balloon-tipped catheter filled with diluted gadolinium-based contrast agent, devices that are currently used clinically for purposes of right heart catheterization (Ratnayaka et al. 2013). However, limitations include the inability to visualize the catheter shaft (Fig. 3a). Moreover, while adjusting the saturation resulted in an increase in signal emanating from the balloon, there was a loss in visualization of anatomical structures (Fig. 3b). In another study, we examined an FDA approved guidewire specifically dedicated for use in MRI, the 0.035" MRWire EmeryGlide (Nano4Imaging GmbH, Aachen, DE) with discrete markers consisting of carboxydextran-coated SPIO nanoparticles (Resovist®) at 0, 2, 4 cm from the tip. The device generated a very robust signal under MRI from the three markers (data not shown). While these examples highlight the ongoing pursuit of MRI-suitable devices, commercially-available catheters and interventional instruments for use in iCMR remain scarce. At the present, the design and development of iCMR-suitable passive and active catheter-based platforms remains largely within the academic arena, with several notable examples from research groups. Kocaturk et al. developed an active, clinical-grade guidewire with a loop and dipole antenna to visualize the tip and shaft of the guidewire, respectively (Kocaturk et al. 2009). The resulting guidewire maintained the mechanical properties of commercially-available x-ray guidewires and was visible under MRI. Magnusson et al. designed a catheter containing a hyperpolarized ^{13}C contrast agent under flow with the ability to visualize the entire catheter length (Magnusson et al. 2007). Lastly, Unal et al. applied gadolinium-based coatings to commercially available catheters and guidewires and were able to image these devices in the canine aorta (Unal et al. 2006).

Herein, our goal was to functionalize several commercially-available endovascular instruments with an SPIO polymer coating for purposes of iCMR. Given that the polymer-jacketed wire guides did not generate significant artifact, we successfully functionalized these such that an SPIO-coated tip could be visualized in arterial anatomy, allowing for safe navigation of these wire guides in vivo in iCMR (Fig. 4b). Balloon catheters of a wide spectrum of sizes were also functionalized and visualized under MRI (Fig. 4d). Previous studies have shown the potential that iCMR has for stent deployment. Raval et al. demonstrated the use of active catheters for accurate stent deployment under real-time MR imaging in a porcine model of aortic coarctation (Raval et al. 2005). We sought to develop a basic stent delivery system based on cobalt stents that: 1) did not cause CMR image distortion (in contrast to stainless steel), which was demonstrated in Fig. 5a and b; and 2) could be visualized during and after deployment. Incorporating a layer of SPIO-functonalized ePTFE into the cobalt stent platform resulted in an iCMR-visible endovascular stent graft, which we successfully deployed in the abdominal aorta of a pig (Fig. 5c-d).

During the course of the study, development of devices suitable for MRI use highlighted important advantages for iCMR. Selective contrast injection for angiography is standard before stent deployment in fluoroscopy. This often requires larger-sized catheters for purposes of injecting contrast around the stent delivery system, or for more vascular access points to inject contrast from a separate catheter. This was wholly unnecessary in the iCMR environment, potentially reducing the risk of vascular complications. For example, while transcatheter aortic valve replacement (TAVR) is typically guided by repeated contrast angiography through a second arterial catheter placed via second arterial access site, TAVR could be performed under real-time CMR, with positioning check before deployment and functional assessment after deployment using high-resolution cine sequences, all without the need for simultaneous contrast injection or additional arterial access. Additionally, iCMR allows for depth perception, as well as measurement of physiologic flow data during the intervention.

While promising, limitations to development of iCMR-suitable devices exist. A major limitation is the use of a non-braided catheter, which results in loss of torqueability, trackability in tortuous vessels, and the potential to kink the catheter. The development of non-ferrous braiding materials that can be incorporated within devices and still provide the requisite mechanical properties can surmount this challenge. Likewise, catheter shape selection to optimize cannulation and back-up support is extremely limited as most high-performance catheters utilize a metal-braid construction. The present study did not evaluate heating of functionalized wire guides, catheters, angioplasty balloons, or stents, but will be an important consideration upon clinical translation. Moreover, current real-time iCMR has significant time and spatial resolution limitations. As a result, the potential utility of iCMR is unlikely to extend to small vessel interventions such as coronary angioplasty. Regardless of these challenges, it is our belief that iCMR represents a safe and accurate modality for cardiovascular interventions, and this study contributes to the burgeoning field by highlighting the feasibility of performing iCMR through incorporation of MRI-visible design considerations to endovascular devices.

5 Conclusions

iCMR has tremendous potential to revolutionize catheter-based interventional cardiovascular procedures, with significant advantages over present-day x-ray fluoroscopy, which remains the clinical gold standard. However, translating iCMR into a clinical reality is principally limited by the lack of MRI-visible endovascular tools and devices. Herein, we demonstrated that SPIO functionalization of a basic set of endovascular instruments, including wire guides and catheters, allowed for active visualization under real-time MRI.

The ability to image these devices in an MRI setting resulted in superior navigation in cardiovascular structures, as well as the ability to perform interventions such as stent deployment. The spatial and temporal resolution provided by MRI, and the potential to visualize these instruments across multiple planes, resulted in enhanced awareness of catheter and stent placement. The capability of performing interventions without the use of x-ray fluoroscopy is expected to eliminate radiation exposure, allowing for procedures to be performed in a wider cohort of patients (e.g. pregnant women, children) and also encourage the pursuit of novel, minimally-invasive cardiovascular interventions. Although MR acquisition is typically slower than fluoroscopy due to factors such as lower frame rate and the need for breath-hold, future experiments will consist of improving image quality and speed of acquisition, and will aim to take advantage of the power of real-time 3D imaging and physiologic flow data during interventions. It is our belief that incorporation of MRI-visible components in endovascular tools will contribute immensely towards translating iCMR into routine clinical practice. Our findings demonstrate the feasibility of iCMR if endovascular tools include design considerations for the MRI environment, and we believe this study will contribute towards continued research in the field of MRI-visible endovascular device development.

Acknowledgements The authors thank Matthew G. Landry for assistance with schematics. This work was supported by the George and Angelina Kostas Research Center for Cardiovascular Nanomedicine. CHL acknowledges support from the Houston Methodist Specialty Physician Group Grant Program. VS-I is grateful for support from the Instituto Tecnológico y de Estudios Superiores de Monterrey and the Consejo Nacional de Ciencia y Tecnología (CONACyT, 490202/278979). MF gratefully acknowledges support from the Ernest Cockrell Jr. Presidential Distinguished Chair at the Houston Methodist Research Institute. MF serves on the Board of Directors of Arrowhead Pharmaceuticals. The authors declare that they have no conflict of interest.

References

M. Andreucci, T. Faga, R. Serra, G. De Sarro, A. Michael, Update on the renal toxicity of iodinated contrast drugs used in clinical medicine. Drug Healthc. Patient Saf. **9**, 25–37 (2017)

C.J. Bakker, R.M. Hoogeveen, J. Weber, J.J. vanVaals, M.A. Viergever, W.P. Mali, Visualization of dedicated catheters using fast scanning techniques with potential for MR-guided vascular interventions. Magn. Reson. Med. **36**(6), 816–820 (1996)

E.J. Benjamin, S.S. Virani, C.W. Callaway, A.M. Chamberlain, A.R. Chang, S. Cheng, et al., Heart disease and stroke Statistics-2018 update: A report from the American Heart Association. Circulation **137**(12), e67–e492 (2018)

A. Berrington de Gonzalez, S. Darby, Risk of cancer from diagnostic X-rays: Estimates for the UK and 14 other countries. Lancet **363**(9406), 345–351 (2004)

T.M. Bhat, M.E. Afari, L.A. Garcia, Atherectomy in peripheral artery disease: A review. J Invasive Cardiol **29**(4), 135–144 (2017)

M. Bock, S. Volz, S. Zuhlsdorff, R. Umathum, C. Fink, P. Hallscheidt, et al., MR-guided intravascular procedures: Real-time parameter control and automated slice positioning with active tracking coils. J. Magn. Reson. Imaging **19**(5), 580–589 (2004)

M. Bock, R. Umathum, S. Zuehlsdorff, S. Volz, C. Fink, P. Hallscheidt, et al., Interventional magnetic resonance imaging: An alternative to image guidance with ionising radiation. Radiat. Prot. Dosim. **117**(1–3), 74–78 (2005)

C.E. Chambers, K.A. Fetterly, R. Holzer, P.J. Lin, J.C. Blankenship, S. Balter, et al., Radiation safety program for the cardiac catheterization laboratory. Catheter. Cardiovasc. Interv. **77**(4), 546–556 (2011)

H. Clogenson, J. Dobbelsteen, Catheters and guidewires for interventional MRI: Are we there yet? J Imaging Intervent Radiol **2**, 28 (2016)

Z.C. Higgs, D.A. Macafee, B.D. Braithwaite, C.A. Maxwell-Armstrong, The Seldinger technique: 50 years on. Lancet **366**(9494), 1407–1409 (2005)

T. Klemm, S. Duda, J. Machann, K. Seekamp-Rahn, L. Schnieder, C.D. Claussen, et al., MR imaging in the presence of vascular stents: A systematic assessment of artifacts for various stent orientations, sequence types, and field strengths. J. Magn. Reson. Imaging **12**(4), 606–615 (2000)

O. Kocaturk, A.H. Kim, C.E. Saikus, M.A. Guttman, A.Z. Faranesh, C. Ozturk, et al., Active two-channel 0.035″ guidewire for interventional cardiovascular MRI. J. Magn. Reson. Imaging **30**(2), 461–465 (2009)

J.J. Krueger, P. Ewert, S. Yilmaz, D. Gelernter, B. Peters, K. Pietzner, et al., Magnetic resonance imaging-guided balloon angioplasty of coarctation of the aorta: A pilot study. Circulation **113**(8), 1093–1100 (2006)

S. Krueger, S. Schmitz, S. Weiss, D. Wirtz, M. Linssen, H. Schade, et al., An MR guidewire based on micropultruded fiber-reinforced material. Magn. Reson. Med. **60**(5), 1190–1196 (2008)

J. Lotz, Interventional vascular MRI: Moving forward. Eur. Heart J. **34**(5), 327–329 (2013)

Y. Ma, N. Gogin, P. Cathier, R.J. Housden, G. Gijsbers, M. Cooklin, et al., Real-time x-ray fluoroscopy-based catheter detection and tracking for cardiac electrophysiology interventions. Med. Phys. **40**(7), 071902 (2013)

P. Magnusson, E. Johansson, S. Mansson, J.S. Petersson, C.M. Chai, G. Hansson, et al., Passive catheter tracking during interventional MRI using hyperpolarized 13C. Magn. Reson. Med. **57**(6), 1140–1147 (2007)

J.R. Mazal, T. Rogers, W.H. Schenke, A.Z. Faranesh, M. Hansen, K. O'Brien, et al., Interventional-cardiovascular MR: Role of the interventional MR technologist. Radiol. Technol. **87**(3), 261–270 (2016)

M.E. Miquel, S. Hegde, V. Muthurangu, B.J. Corcoran, S.F. Keevil, D.L.G. Hill, et al., Visualization and tracking of an inflatable balloon catheter using SSFP in a flow phantom and in the heart and great vessels of patients. Magn. Reson. Med. **51**(5), 988–995 (2004)

R.A. Omary, O. Unal, D.S. Koscielski, R. Frayne, F.R. Korosec, C.A. Mistretta, et al., Real-time MR imaging-guided passive catheter tracking with use of gadolinium-filled catheters. J. Vasc. Interv. Radiol. **11**(8), 1079–1085 (2000)

T. Pucelikova, G. Dangas, R. Mehran, Contrast-induced nephropathy. Catheter. Cardiovasc. Interv. **71**(1), 62–72 (2008)

K. Ratnayaka, A.Z. Faranesh, M.A. Guttman, O. Kocaturk, C.E. Saikus, R.J. Lederman, Interventional cardiovascular magnetic resonance: still tantalizing. J. Cardiovasc. Magn. Reson. **10**, 62 (2008)

K. Ratnayaka, A.Z. Faranesh, M.S. Hansen, A.M. Stine, M. Halabi, I.M. Barbash, et al., Real-time MRI-guided right heart catheterization in adults using passive catheters. Eur. Heart J. **34**(5), 380–389 (2013)

A.N. Raval, J.D. Telep, M.A. Guttman, C. Ozturk, M. Jones, R.B. Thompson, et al., Real-time magnetic resonance imaging-guided

stenting of aortic coarctation with commercially available catheter devices in Swine. Circulation **112**(5), 699–706 (2005)

T. Rogers, K. Ratnayaka, J.M. Khan, A. Stine, W.H. Schenke, L.P. Grant, et al., CMR fluoroscopy right heart catheterization for cardiac output and pulmonary vascular resistance: Results in 102 patients. J. Cardiovasc. Magn. Reson. **19**(1), 54 (2017)

D.L. Rubin, A.V. Ratner, S.W. Young, Magnetic-susceptibility effects and their application in the development of new ferromagnetic catheters for magnetic-resonance-imaging. Investig. Radiol. **25**(12), 1325–1332 (1990)

M. Saeed, S.W. Hetts, J. English, M. Wilson, MR fluoroscopy in vascular and cardiac interventions (review). Int. J. Card. Imaging **28**(1), 117–137 (2012)

C.E. Saikus, R.J. Lederman, Interventional cardiovascular magnetic resonance imaging: A new opportunity for image-guided interventions. JACC. Cardiovasc. Imaging **2**(11), 1321–1331 (2009)

K. Slicker, W.G. Lane, O.O. Oyetayo, L.A. Copeland, E.M. Stock, J.B. Michel, et al., Daily cardiac catheterization procedural volume and complications at an academic medical center. Cardiovasc. Diagn. Ther. **6**(5), 446–452 (2016)

A. Stadler, W. Schima, A. Ba-Ssalamah, J. Kettenbach, E. Eisenhuber, Artifacts in body MR imaging: Their appearance and how to eliminate them. Eur. Radiol. **17**(5), 1242–1255 (2007)

O. Unal, J. Li, W. Cheng, H. Yu, C.M. Strother, MR-visible coatings for endovascular device visualization. J. Magn. Reson. Imaging **23**(5), 763–769 (2006)

K. Zhang, A.J. Krafft, R. Umathum, F. Maier, W. Semmler, M. Bock, Real-time MR navigation and localization of an intravascular catheter with ferromagnetic components. Magn Reson Mater Phy **23**(3), 153–163 (2010)

Publisher's note Springer Nature remains neutral with regard to jurisdictional claims in published maps and institutional affiliations.